# Boosting the energy storage performance of BCZT-based capacitors by constructing the Schottky contact

*Zixiong Sun[ac*], Haoyang Xin[a], Liming Diwu[a], Zhanhua Wang[b*], Ye Tian[c], Hongmei Jing[d], Xiuli Wang[e], Wanbiao Hu[f], Yongming Hu[g*], Zhuo Wang[c*]*

*a School of Electronic Information and Artificial Intelligence, Shaanxi University of Science and Technology, Xi'an 710021, PR China.*

*b State Key Laboratory of Polymer Materials Engineering (Sichuan University), Chengdu, 610065, PR China.*

*c School of Materials Science and Engineering, Shaanxi University of Science and Technology, Xi'an 710021, PR China.*

*d School of Physics and Information Technology, Shaanxi Normal University, Xi'an, 710119, PR China*

*e Engineering Research Center of Eco-friendly Polymeric Materials, Ministry of Education, (Sichuan University), Chengdu, 610065, PR China*

*f Yunnan Key Laboratory of Electromagnetic Materials and Devices, Yunnan, 650000, PR China*

*g Hubei Key Laboratory of Micro-Nanoelectronic Materials and Devices, Hubei University, Wuhan 430062, China*

---

**Corresponding author: Zixiong Sun, Zhanhua Wang, Yongming Hu, Zhuo Wang.*

*E-mail address: sunzx@sust.edu.cn; zhwangpoly@scu.edu.cn; huym@hubu.edu.cn, wangzhuo@sust.edu.cn.*

# *Supplementary Information*

## 1. Experimental Section

### *1.1 Thin film's deposition*

Stoichiometric targets of $Ba_{0.7}Ca_{0.3}Zr_{0.2}Ti_{0.8}O_3$ (BCZT) and Nb-doped $SrTiO_3$ (NSTO) (001) substrates were sourced from MTI (KJ Group). The same target was used for the growth of both BCZT and BCZT-$_{OD}$ layers, with the target surface manually polished using sandpaper, followed by cleaning with a nitrogen gun to remove any residue. The BCZT layer was grown by pulsed laser deposition (PLD) at 800 °C under an oxygen pressure of 0.2 mbar, utilizing a KrF excimer laser with a frequency of 5 Hz. For the BCZT-$_{OD}$ layer, the same growth conditions were used, except the oxygen pressure was reduced to 0.01 mbar to introduce oxygen vacancies. Following deposition, an in-situ annealing process was conducted at 800 °C under an oxygen pressure of 400 mbar in the same chamber. The thickness of each sublayer was controlled through deposition time, resulting in a thickness of approximately 150 nm for the BCZT-$_{OD}$ layer and 450 nm for the BCZT layer, making the total film thickness around 600 nm. A top electrode of gold (Au) with a thickness of approximately 100 nm was then deposited using sputtering.

### *1.2 Characterization*

X-ray diffraction analysis was performed using a PANalytical X'Pert³ MRD diffractometer, employing $2\theta$-$\omega$ scans, phi-scans, X-ray reflectivity, and reciprocal space mapping (RSM). For $2\theta$-$\omega$ scans, the step size and time per step were set to 0.0005° and 0.5 seconds, respectively. For RSM mappings, both the $2\theta$ and $\omega$ axes used

a step size of 0.02°, with a time per step of 20 seconds for the $2\theta$ axis. Scanning electron microscopy (SEM) images were captured using a ZEISS MERLIN HR-SEM system with secondary electron imaging. Compositional analysis was conducted with the attached Energy Dispersive Spectroscopy (EDS) module under high vacuum conditions. The dielectric permittivity ($\varepsilon$-$f$) and loss tangent ($tan\delta$-$f$) curves, along with $I$-$V$ results, were collected using a Keithley 4200 LCR meter. Dielectric constants were calculated based on the formula $C = \frac{\varepsilon S}{4k\pi d}$. $I$-$V$ measurements followed a top-to-bottom configuration, as shown in Fig. S2. Ferroelectric hysteresis ($P$-$E$) loops were measured using an *aixACCT TF2000E* ferroelectric tester in unipolar mode at 1000 Hz.

## 2. Calculation of *ESD* and $\eta$

The energy storage density($W_{rec}$) and $\eta$ of a dielectric capacitor under a specific applied electrical field ($E$) can be represented by the following formula:

$$W_{\text{rec}} = \int_{P_{\text{m}}}^{P_{\text{r}}} E\text{d}P \qquad \text{Eq. S1}$$

$$W_{\text{char}} = \int_{0}^{P_{\text{m}}} E\text{d}P \qquad \text{Eq. S2}$$

$$\eta = W_{rec}/W_{sto}100\% \qquad \text{Eq. S3}$$

in which the $W_{rec}$ and $W_{char,}$ are the amount of energy stored per unit volume and energy-charged density(ECD) during one charge-discharge process, respectively. $P$ is the generated polarization under $E$, and the $P_m$ and $P_r$ are the maximum polarization upon charging and the remanent polarization when the electrical field returns to zero, respectively.

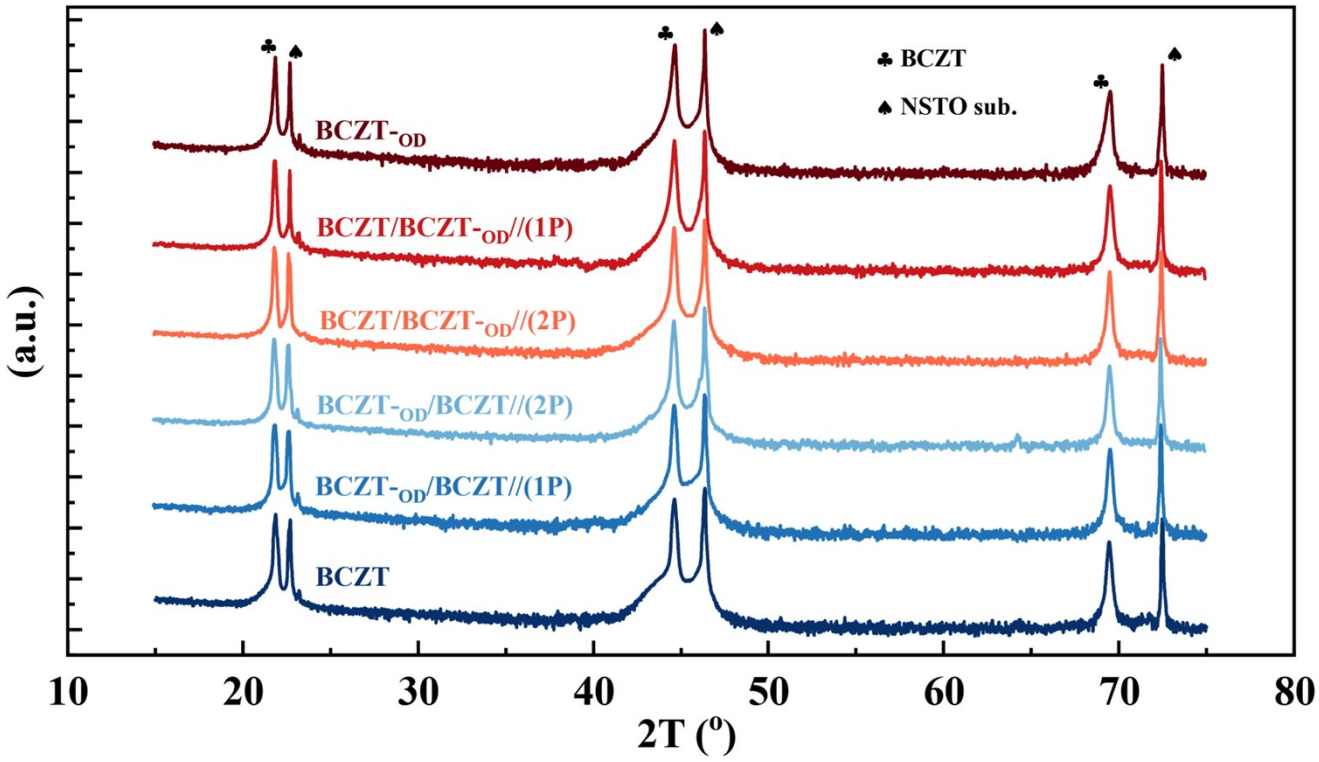


*Figure S1 XRD 2Theta-ω-scans from 15° to 75° for all films.*

3. ***Gaussian-LorenCross*** **function:**

$$y = y_0 + \frac{A}{1 + \frac{e^{\frac{0.5(1 - s)(x - x_c)^2}{w^2}}}{\frac{s(x - x_c)^2}{w^2}}} \qquad \text{Eq. S4}$$

The $y_0$, $x_c$, $A$, $w$, and $s$ are the base, center, amplitude, width, and shape of each peak, respectively. The maximum number of iterations and the tolerance of the fitting process are 200 and $1e^{-6}$, respectively, which indicate very high reliability.

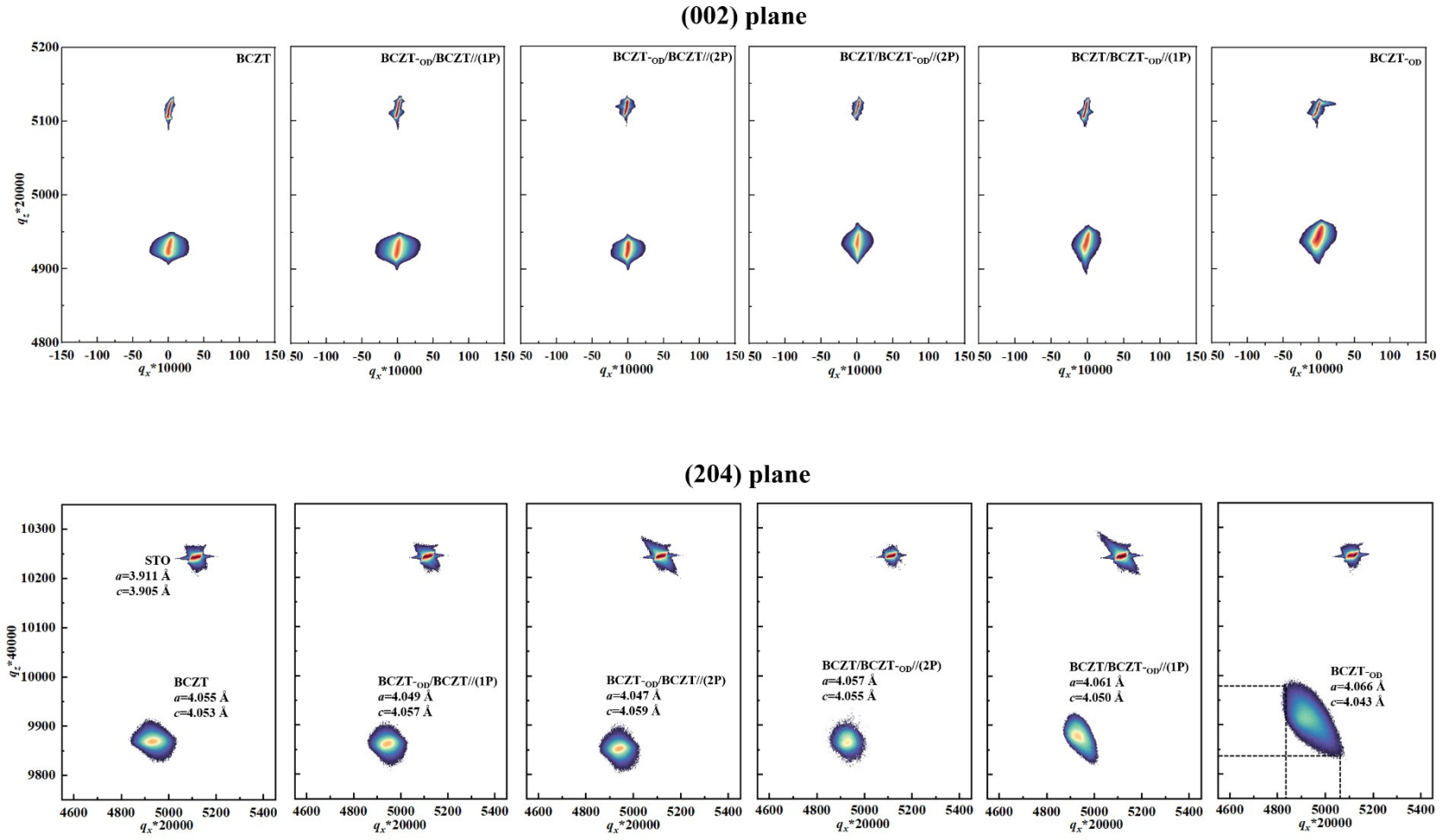


*Figure S2 RSM mappings of all films around (002) plane and (204) plane.*

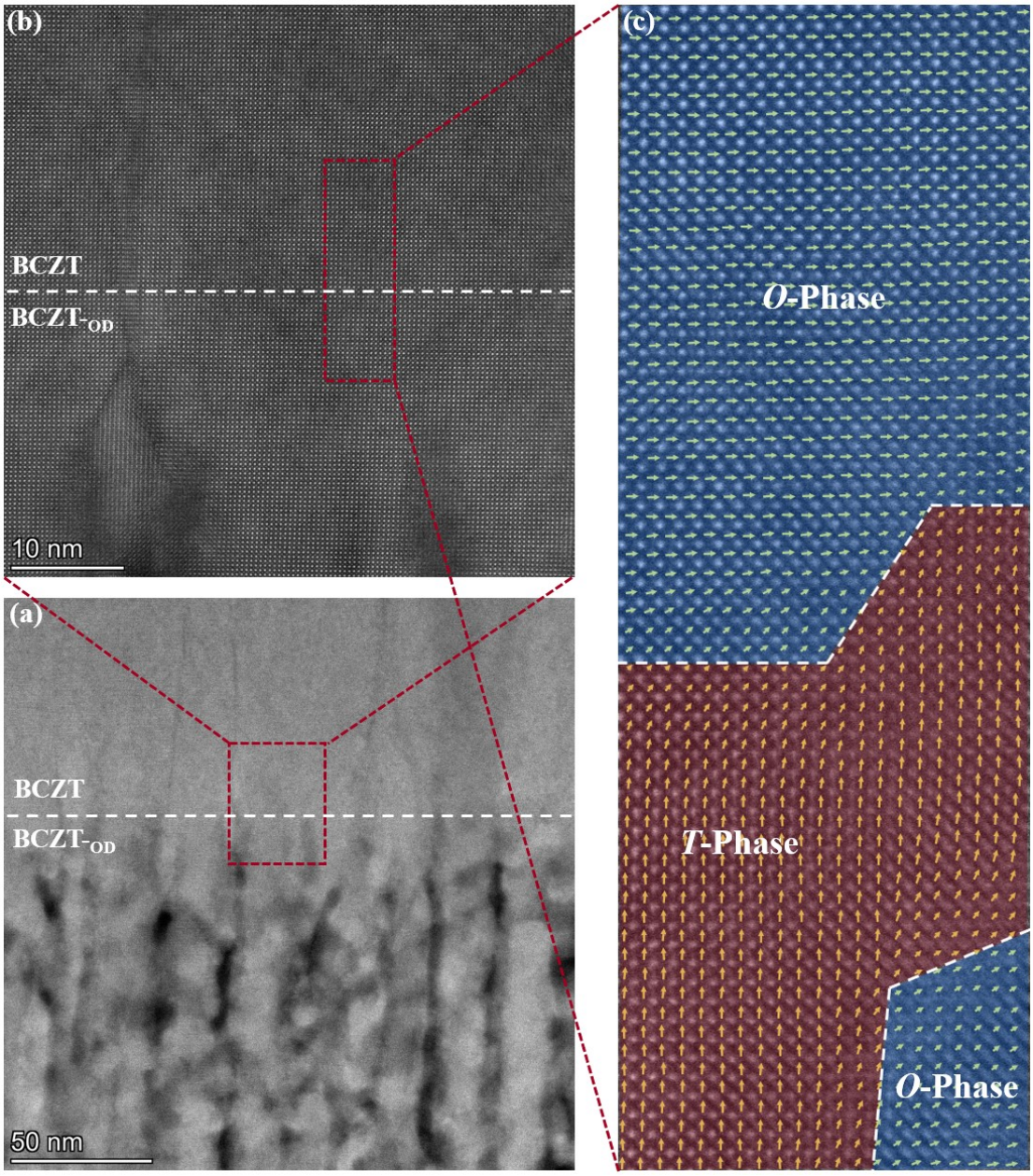


*Figure S3 (a) The enlarged-view of the red dashed area in Figure 3(f2); (b) the enlarged-view of the red dashed area in Figure S3(a), in which no obvious interface can be seen between the BCZT layer and the BCZT-$_{OD}$ layer; (c) the enlarged-view of the red dashed area in Figure S3(b), and the phase distribution can be clearly seen.*

## 4. *Weibull* distribution

Before calculating the energy storage density ($W_{rec}$), the electric breakdown strength ($E_b$) of each film should be confirmed by employing the *Weibull* distribution, which can be expressed as follows:

$$X_i = \ln E_i \quad \text{Eq. S5}$$

$$Y_i = \ln( - \ln (1 - P_i)) \quad \text{Eq. S6}$$

$$P_i = \frac{i}{1 + n} \quad \text{Eq. S7}$$

where $X_i$ and $Y_i$ are the two parameters of the Weibull distribution, $Y_i$ varies linearly with $X_i$ with a slope of $\beta$, $E_i$, and $P_i$ are the sample's breakdown field and the electric field's failure probability distribution, respectively. While $n$, $i$, and $\beta$ are the total number of specimens, the serial number of dielectric strength, and the slope of the linear relationship between $\ln(E_i)$ and $\ln(-\ln(1-P_i))$, respectively.

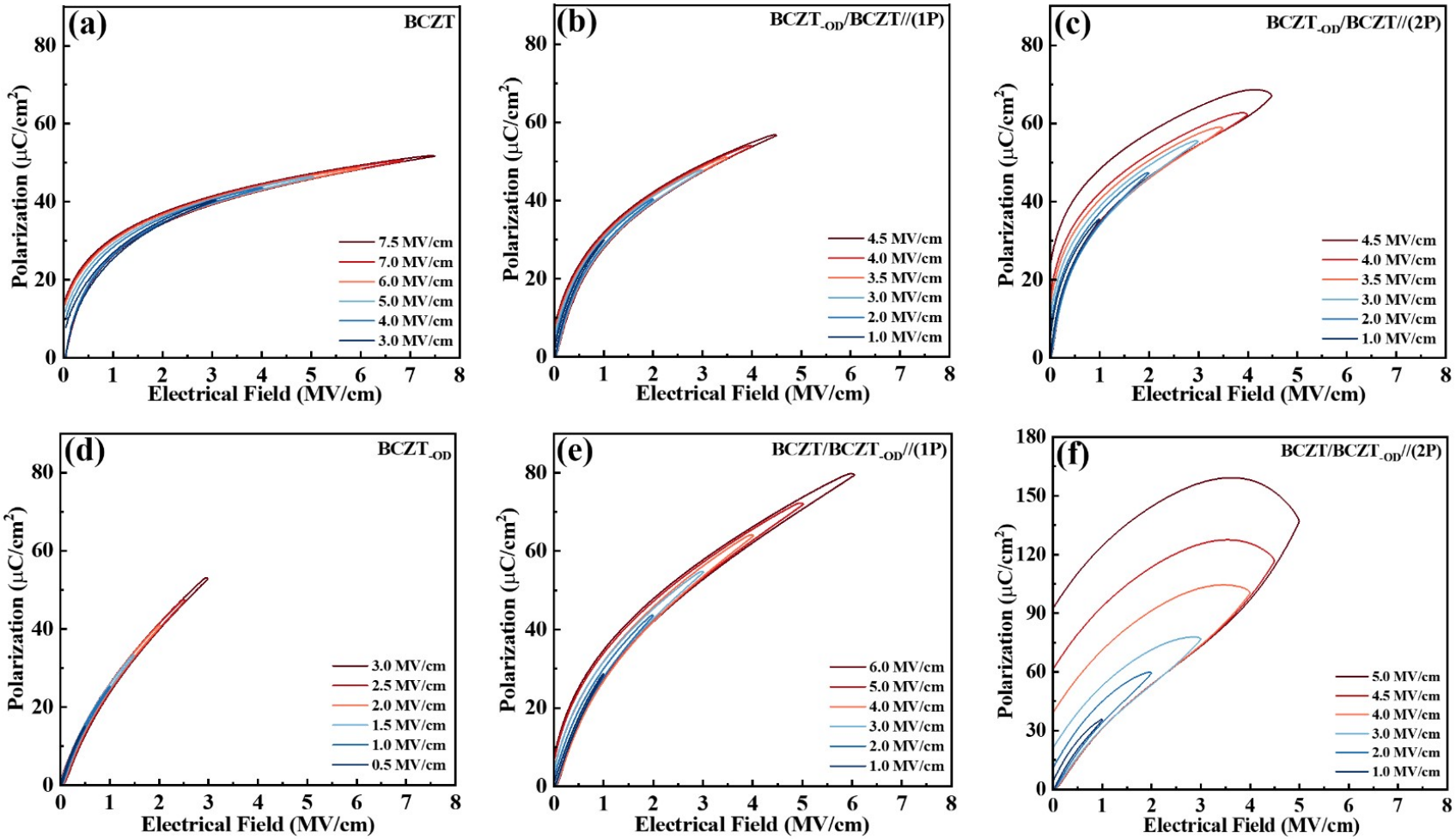


*Figure S4 unipolar P-E loops all films at different electric fields.*

## 5. Working principle of the PFM

As shown in Figure S4, it operates by applying an AC voltage through a conductive tip in contact with the films' surface. This induces a piezoelectric response in films with a non-centrosymmetric structure, causing local mechanical deformation (expansion or contraction) in response to the applied electric field. The PFM tip detects this deformation through deflections of the cantilever, which are measured using a laser beam reflected off the cantilever surface. The deflection signals provide information about the sample's piezoelectric properties, polarization orientation, and switching behavior, enabling the mapping of domain structures and electromechanical activity at the nanoscale.

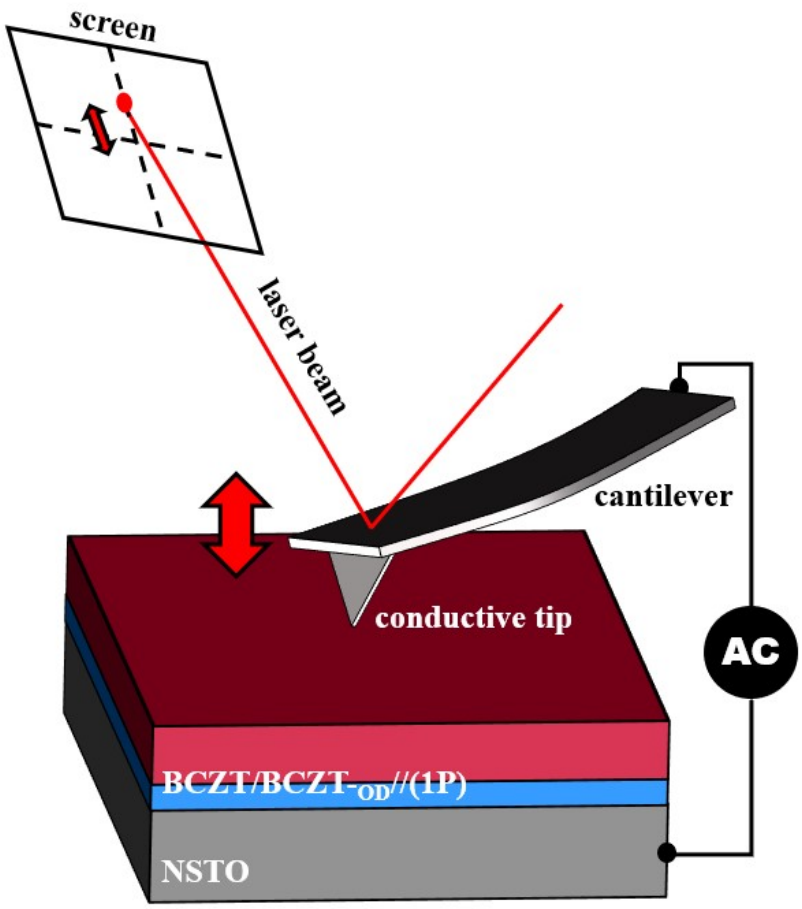


*Figure S5 Working principle of the piezoresponse force microscopy*

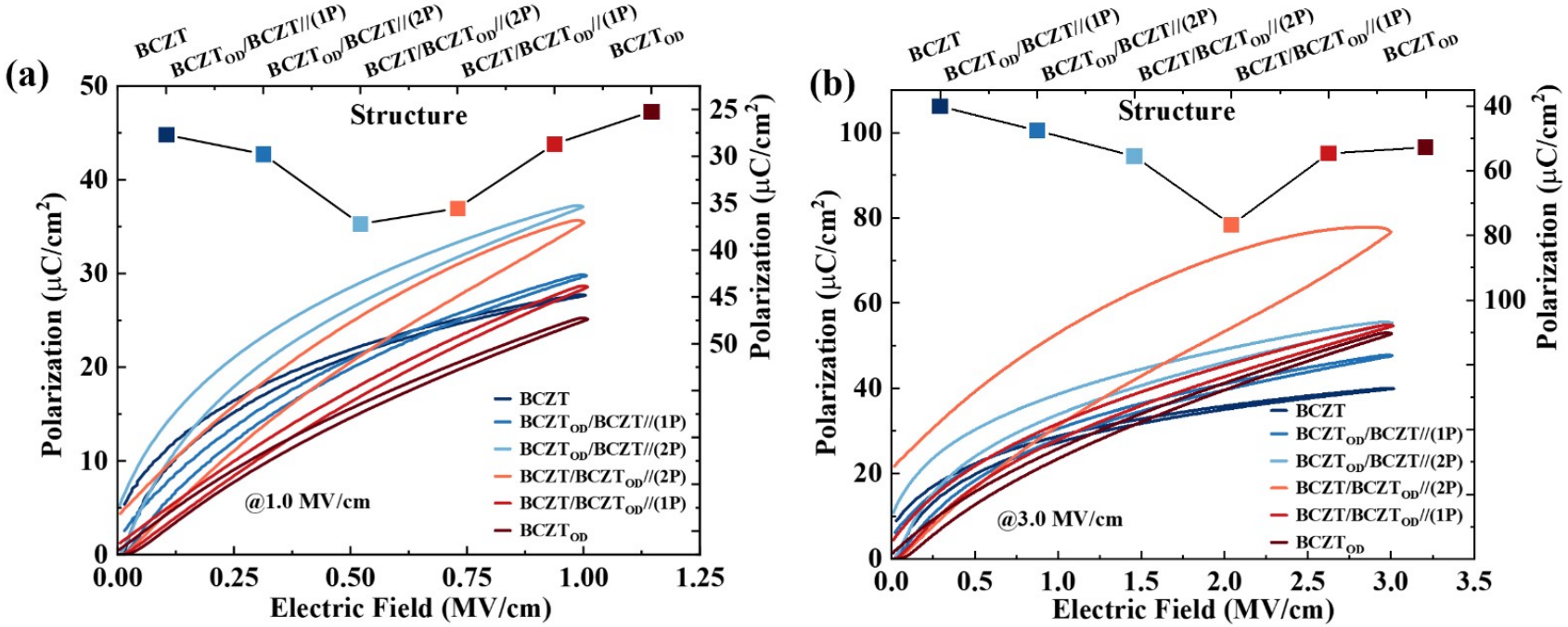


*Figure S6 unipolar P-E loops of all the films at (a) 1.0 MV/cm; (b) 3.0 MV/cm with their corresponding $P_{max}$.*

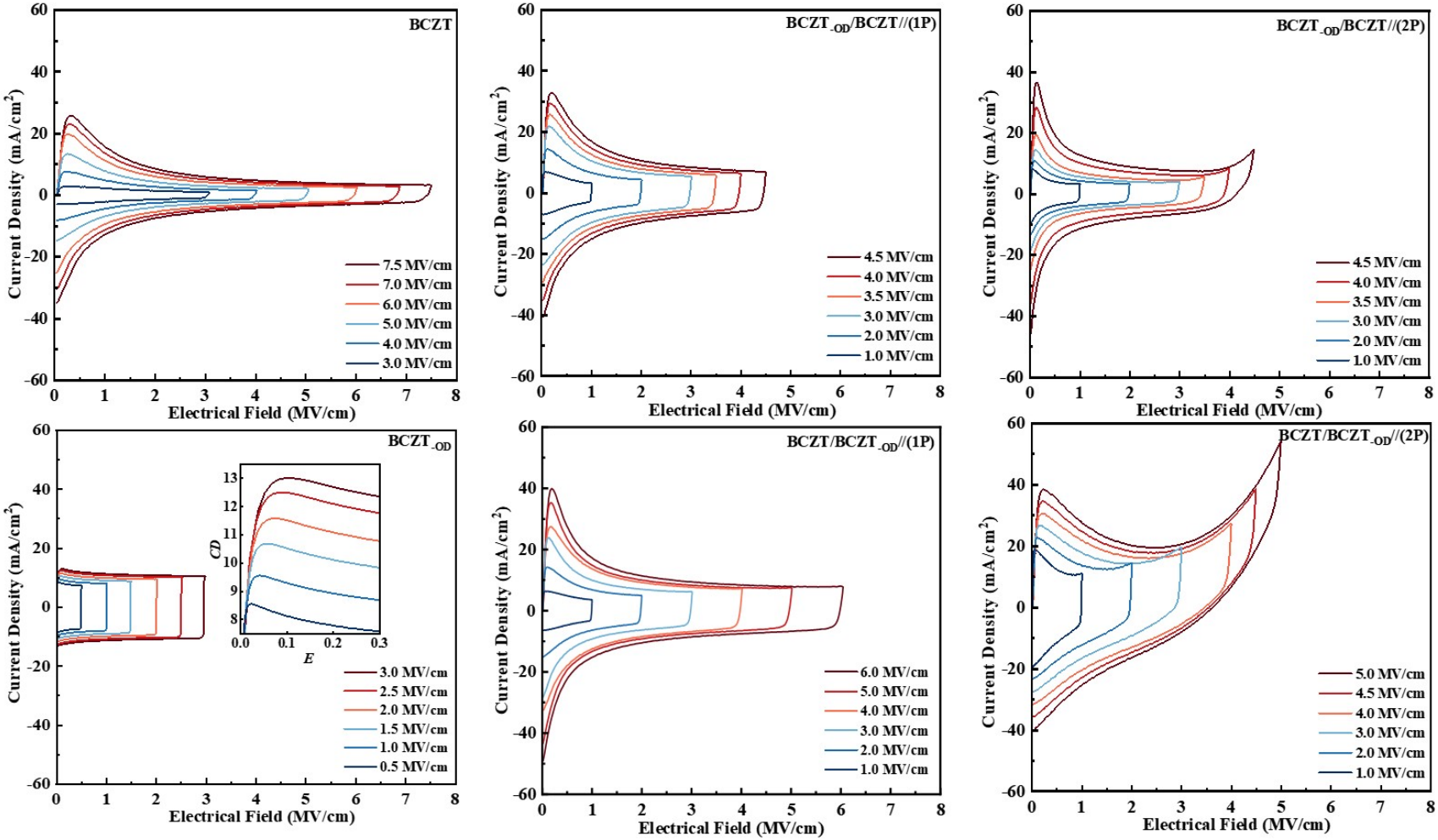


*Figure S7 unipolar J-E curve of all the films at different electric fields*

## 6. Discussion of the contribution of the dipole polarization

In this work, the dipole polarization ($P_{dn}$), which resulted from the formation of the defect dipoles of $V_O^{\cdot\cdot} - Ti^{3+}$ and $V_O^{\cdot\cdot} - Zr^{3+}$, mostly exist in the BCZT-$_{OD}$ layer. According to the definition of dipole moment ($p$), which is expressed below:

$$p = \varepsilon_0 \alpha E_{local} = ql \quad \text{Eq. S8}$$

in which the $E_{local}$, $q$, and $l$ are the electrical field applied on each unit cell, charge of the dipole and the distance between the center of the positive charge and the center of the negative charge in the dipole, respectively. Combine it with the relationship between the polarization and the applied electric field, which is expressed be low:

$$P = (\varepsilon_r - 1)\varepsilon_0 E = N\alpha E \quad \text{Eq. S9}$$

in which $E$ is the applied external electric field on the dielectric material, and $P$ is the total polarization triggered by $E$. The $\varepsilon_r$ and $\varepsilon_0$ are the material's dielectric constants (or relative permittivity) and the vacuum permittivity, which equals $8.854*10^{-12}$ F/m, respectively. $N$ is the number of induced dipole moments in unit volume, and the $\alpha$ is the polarizability of the dielectric. We can have the following formula below:

$$P_{dn} = \frac{3\varepsilon_r}{\frac{3\varepsilon_0}{N^2 ql} + \frac{2}{E}} \quad \text{Eq. S10}$$

In this work, the contribution of $P_{dn}$ mainly comes from the BCZT-$_{OD}$ layer, and the $q$, $l$, and $N$ should be the same. The $P_{dn}$ should has a positive correlation with the partial voltage.

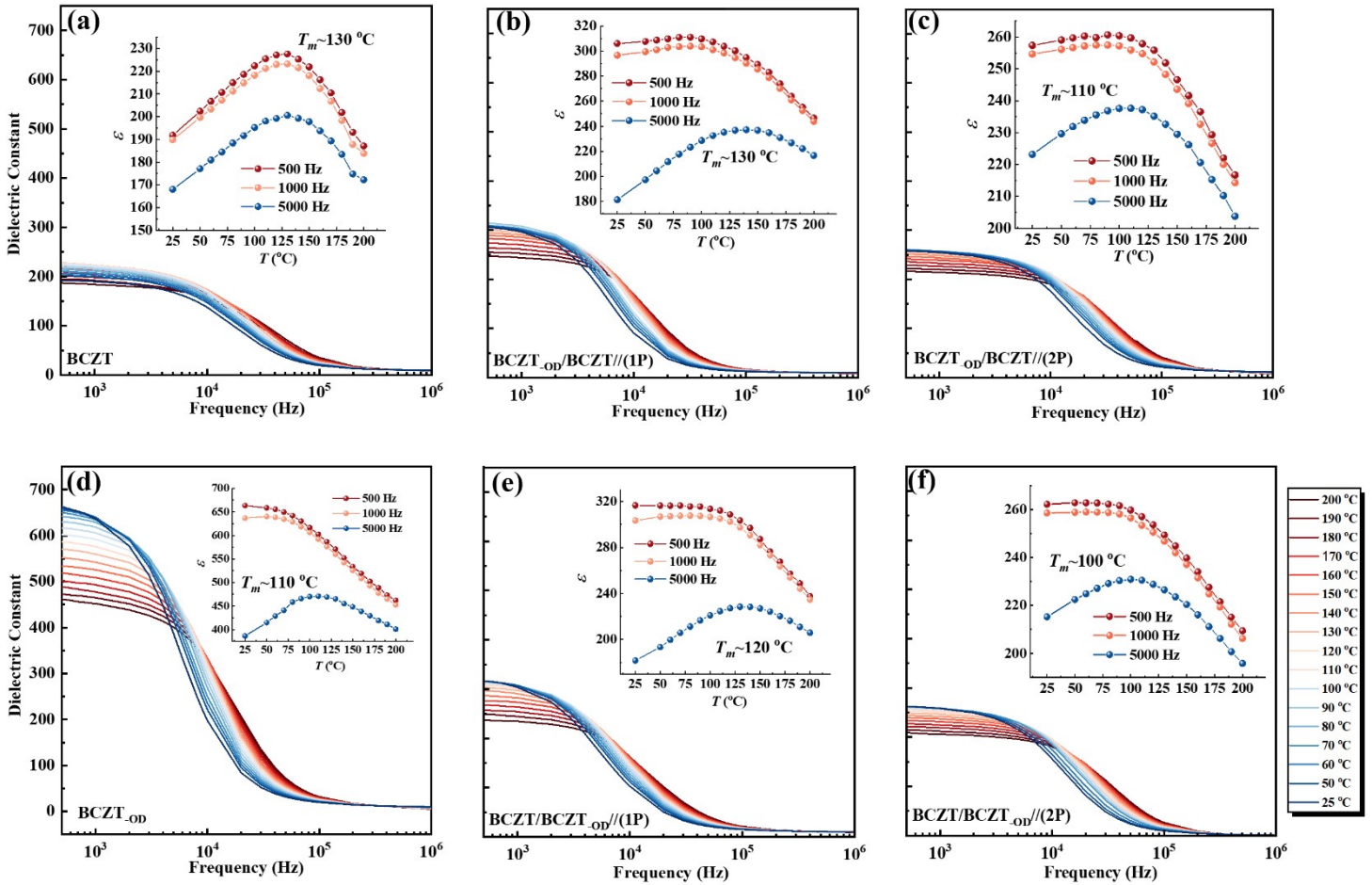


*Figure S8 the frequency dependence of the dielectric constant (ε-f curve) at different temperatures for all films, the temperature dependence of the dielectric constant (ε-T curve), which were extracted from the ε-f curves are inserted in each figure.*

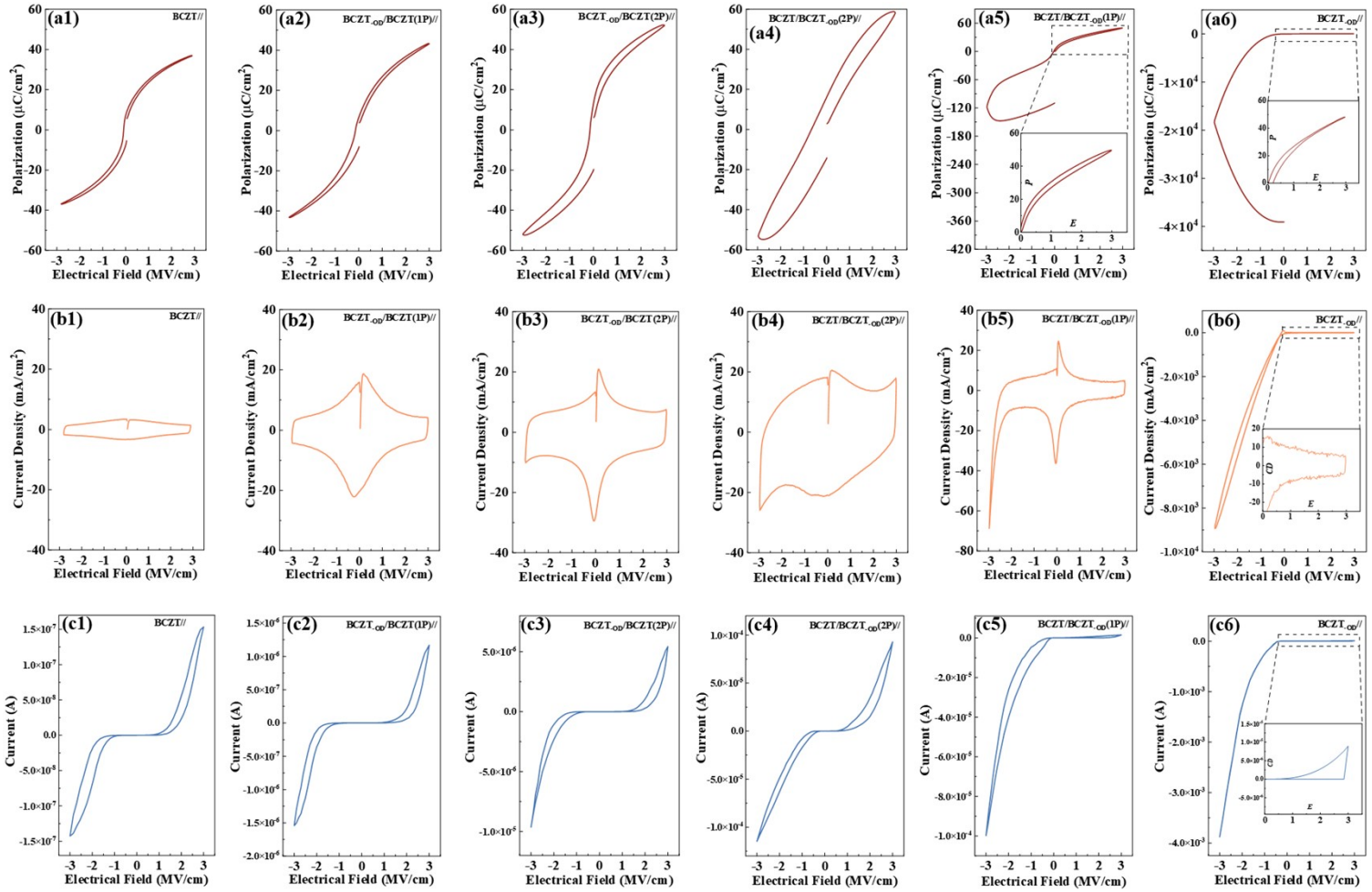


*Figure S9 the (a1)-(a6) bipolar P-E loops of; (b1)-(b6) corresponding J-E curves; (c1)-(c6) I-V characteristics of all the films.*

## 7. Explanation of the *Schottky* barrier formation

Since the NSTO (001) work function (~4.2 eV)[1,2] is higher than the electron affinity of the BCZT-$_{OD}$ (001) (<3.2 eV)[3,4], once connected, the Fermi level of both NSTO and BCZT-$_{OD}$ should be aligned, which leads to band bending in the interface. According to the results of Figure 4(a1), (a2), and (b), the majority of carriers of BCZT-$_{OD}$ are confirmed to be electrons. Thus, the NSTO/BCZT-$_{OD}$ interface can be regarded as the contact between metal and *n*-type semiconductors[5]. Considering the BCZT behaves as a typical dielectric, which won't affect the NSTO/BCZT-$_{OD}$ interface, the band diagram of the NSTO/BCZT-$_{OD}$ interface before and after contact can be depicted as Figure S10 (b1) and (b2), respectively, and the whole device can be defined as a metal-semiconductor-dielectric (MSD) structure. When equilibrium is reached, in this case, the electrons would drift from the BCZT-$_{OD}$ side to the NSTO side and a depletion layer ($R_d$) formed in the NSTO/BCZT-$_{OD}$ interface. More electrons will thus be trapped in $R_d$ and finally, a build-in potential ($\Phi_b$) formed. When applying a forward external voltage ($V$) pointing from BCZT-$_{OD}$ to NSTO, as seen in Fig. S10 (c), the BCZT-$_{OD}$ Fermi level moves down, increasing the $\Phi_b$ to $\Phi_b+V$ and $R_d$ to $R_d'$. In this case, more electrons were trapped in the interface, and the current spread was blocked. When the bias was switched to a reverse one, as seen in Figure S10 (b4), the trapped electrons receive more energy to cross the NSTO/BCZT-$_{OD}$ interface, and the Fermi level of the BCZT-$_{OD}$ moves up, making the electrons easily to flow from the BCZT-$_{OD}$ side to the NSTO side, and thus the current starts to flow.

## 8. The physical meaning of the abbreviations in the band diagram analyzing

$E_{VAC}$: the vacuum level

$E_N$: the Fermi energy level of the NSTO substrate

$E_{FB}$: the Fermi energy level of the BCZT-$_{OD}$ layer

$E_{CB}$: the conduction band of the BCZT-$_{OD}$ layer

$E_{VB}$: the valence band of the BCZT-$_{OD}$ layer

$\Phi_N$: the work function of the NSTO substrate

$\Phi_B$: the work function of the BCZT-$_{OD}$ layer

$\chi_B$: the electron affinity of the BCZT-$_{OD}$ layer

$\Phi_S$: the Schottky barrier height

$\Phi_b$: the build-in potential caused by the band bending

$V$: the external applied voltage

$R_d$: the origin depletion region before the bias applied

$R_d$': the increased depletion region after the bias applied

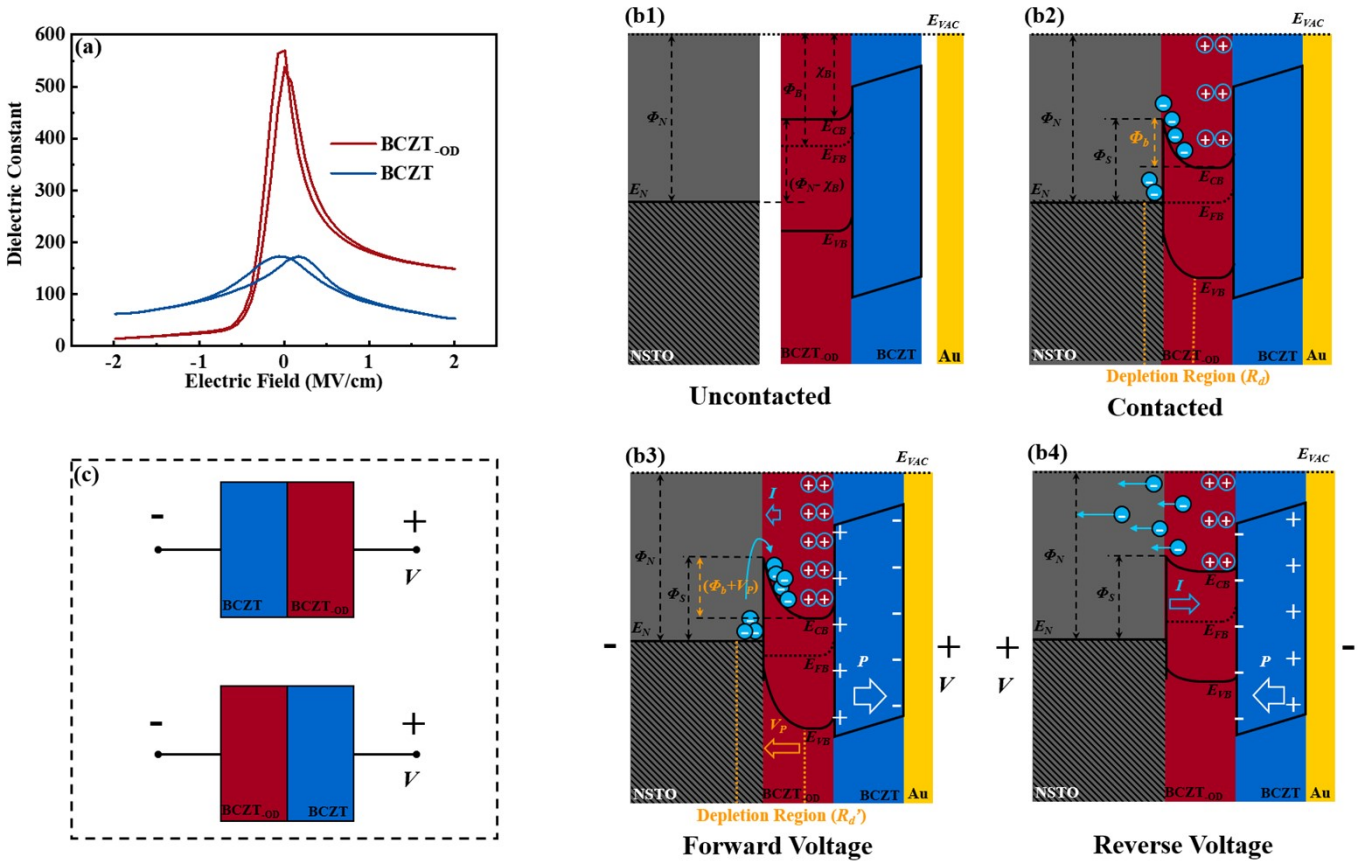


*Figure S10 (a) the ε-V curve of pristine BCZT and BCZT-$_{OD}$ film; the band diagram of the NSTO/BCZT-$_{OD}$ interface of the BCZT/BCZT-$_{OD}$//(1P) (b1) before contact; (b2) after contact; (b3) under forward bias V; (b4) under reverse bias V; (c) the equivalent circuit of BCZT/BCZT-$_{OD}$//(1P) and BCZT-$_{OD}$/BCZT//(1P) under forward bias V.*

**7. Finite Element Simulation**

The *COMSOLMultiphysics6.0* linking with *Matlab5.2* was employed to simulate the potential and electric field distribution and the current spread. Once the breakdown happens, the film will undergo an irreversible transformation, widely believed to be the joint effect of electric and thermal fields. Based on this, the *AC/DC module* and *heat transfer module* in *COMSOLMultiphysics6.0* are both called, and the physical model can be expressed as follows:

The electrical breakdown process was described according to the spread of current density with the boundary conditions meeting:

$$\boldsymbol{n}\cdot\boldsymbol{i}=0 \qquad \text{Eq. S11}$$

where $\boldsymbol{n}$ and $\boldsymbol{i}$ are the normal vector and current density vector, respectively. This boundary condition means that no electric current flows into the boundary. The constitutive relations are expressed as:

$$\boldsymbol{J}=\sigma\boldsymbol{E} \qquad \text{Eq. S12}$$

$$\boldsymbol{J}=A^{*}T^{2}\exp\left[\frac{-q(\emptyset_S-\sqrt{q\boldsymbol{E}/4\pi\varepsilon_r\varepsilon_0})}{kT}\right] \qquad \text{Eq. S13}$$

which is the standard Ohmic's contact and Schottky contact, respectively, and

$$\boldsymbol{D}=\varepsilon_0\varepsilon_r\boldsymbol{E} \qquad \text{Eq. S14}$$

where $\boldsymbol{J}$ and $\boldsymbol{E}$ are the current density and external electrical field, respectively, and $\sigma$ and $\varepsilon_r$ are each material's electrical conductivity and dielectric constant (permittivity), which needs input in the model. $\varepsilon_0$ is vacuum permittivity with a value of $8.854187817*10^{-12}$ F/m. The $A^{*}$, $k$, $q$, $\varepsilon_0$, and $\varepsilon_r$, which won't change with external

factors, are the effective Richardson constant, Boltzmann's constant, electronic charge, vacuum dielectric constant, and relative dielectric constant, respectively. In this work, the Schottky emission (Eq. S13) was applied in the BCZT/BCZT-$_{OD}$//(1P) thin film with the $\Phi_S$ of 1.4 eV, while all the other films were set to obey the Ohmic's contact (Eq. S8).

Considering the stationary equation of continuity of the model after a long time, Eq. S9 and 10 should be changed to a more general form:

$$\boldsymbol{J}=\sigma\boldsymbol{E}+\frac{\partial \boldsymbol{D}}{\partial t}+\boldsymbol{J_e} \qquad \text{Eq. S15}$$

$$\boldsymbol{J}=A^{*}T^{2}\exp\left[\frac{-q(\emptyset_S-\sqrt{q\boldsymbol{E}/4\pi\varepsilon_r\varepsilon_0})}{kT}\right]+\frac{\partial \boldsymbol{D}}{\partial t}+\boldsymbol{J_e} \qquad \text{Eq. S16}$$

At the same time, current conservation should be met from then on with the equations:

$$\nabla\cdot\boldsymbol{J}=Q_{j.v} \qquad \text{Eq. S17}$$

$$\boldsymbol{E}=-\nabla V \qquad \text{Eq. S18}$$

where $Q_{j.v}$ and $\boldsymbol{D}$ represent the change rate of electric charge per unit volume and the electric displacement vector. $\boldsymbol{J_e}$ is the current density and density of the external electric current, and $V$ denotes the electrical potential. Here, we use the *If sentence*, which is written as *if(ht. alpha>0.1,6e6,0.04)* and was input in the software to determine if a breakdown occurred or not. It means if the breakdown happens, the $\sigma$ takes the 6e6; otherwise, it takes 0.04. The *ht. alpha* is the physical name of $\frac{\partial \alpha}{\partial t}$, which represents an anisotropic thermal diffusivity($\alpha$).

The heat transfer in solid interface solves for the following equation derived from:

$$d_z(\rho C_p)_{eff}\frac{\partial T}{\partial t} + d_z(\rho C_p)_{\text{eff}}\boldsymbol{u}\cdot\nabla T + \nabla\cdot\boldsymbol{q} = d_z Q + q_0 + d_z Q_{ted} \quad \text{Eq. S19}$$

in which the $\boldsymbol{u}$ is the fluid velocity vector, and the $\boldsymbol{q}$ is the conductive heat flux that is written as:

$$\boldsymbol{q} = -d_z k_{eff}\nabla T \quad \text{Eq. S20}$$

and the $d_z$, $k_{eff,}$ and $\nabla T$ are the domain thickness in the out-of-plane direction, effective thermal conductivity, and temperature perturbation, respectively. The $(\rho Cp)_{eff}$ is the effective volumetric heat capacity at constant pressure that is composed of two parts:

$$(\rho C_p)_{eff} = \theta_{it}k_{it} + (1 - \theta_{it})k \quad \text{Eq. S21}$$

where the $\theta_{it}$ and $k$ are the fraction of transformation and thermal conductivity, respectively, and the $\theta_{it}$ can be expressed as:

$$\theta it = \min(\alpha_b, 1) \quad \text{Eq. S22}$$

where the $\alpha_b$ is the fraction of film that was broken down to correspond to the whole film. The $Q$ in Eq. S19 is the heat source and is defined as:

$$Q = -\rho L_{it,h}\frac{\partial \theta_{it}}{\partial t}(T > T_{it.h}) \quad \text{Eq. S23}$$

where the $T_{it}$, $t_{it}$, and $L_{it}$ are the transformation temperature, transformation time, and the enthalpy change when the electric breakdown happens.

The following formula should be satisfied when the *heat transfer module* is coupled with the *AC/DC module*.

$$\frac{\partial \alpha}{\partial t} = \frac{1}{t_{it,h}}(T > T_{it,h}) \quad \text{Eq. S24}$$

Once the electric breakdown happens, the $\frac{\partial \alpha}{\partial t}$ changes, so the $\sigma$ mentioned above also

changes. In our work, the $T_{it}$ and $t_{it}$ are set to be 150 $^{o}$C and 0.01ns, respectively, according to the literature. The serial number of the *COMSOLMultiphysics6.0* and *Matlab5.2* is offered by Sichuan University.

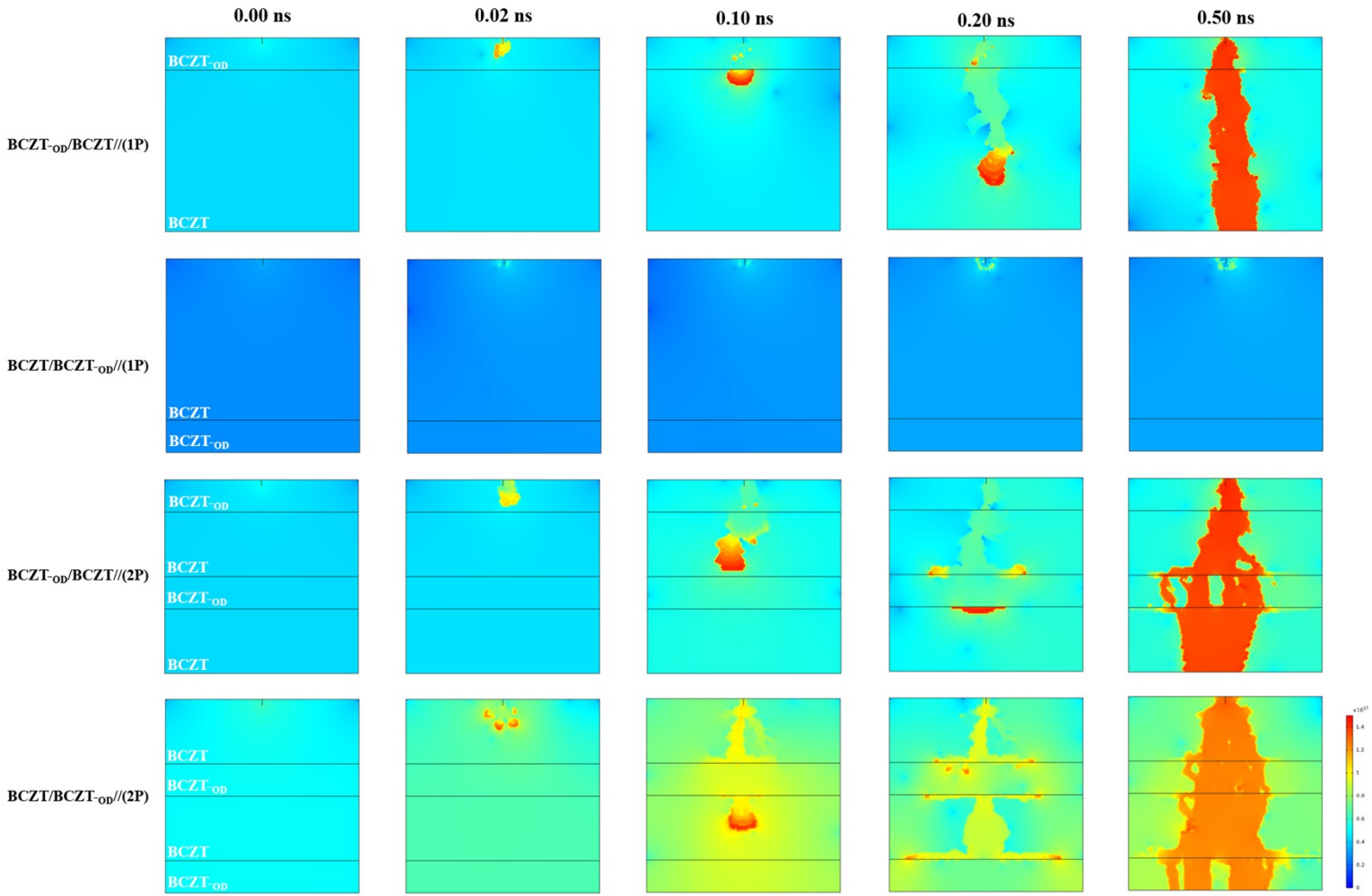


*Figure S11 the electric breakdown process under 6.0 MV/cm of the multilayers simulated by the link of COMSOLMultiphysics6.0 and Matlab5.2 using the FEM.*

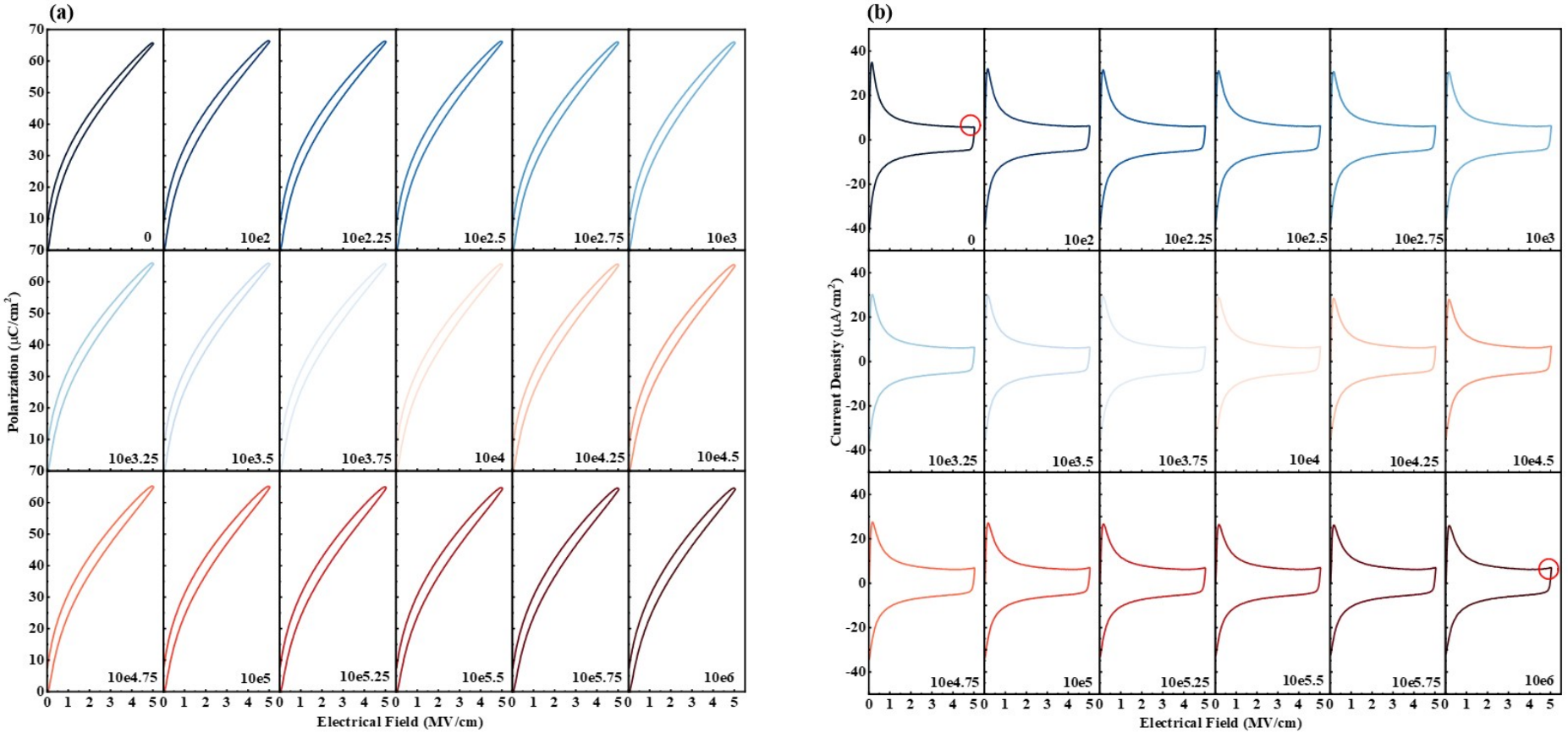


*Figure S12 The (a) P-E loops; (b) J-E curves of the BCZT-/BCZT-$_{OD}$//(1P) during the fatigue process from the 1$^{st}$ circle to the 10$^{6th}$ circle at 1000 Hz at 5.0 MV/cm at room temperature.*

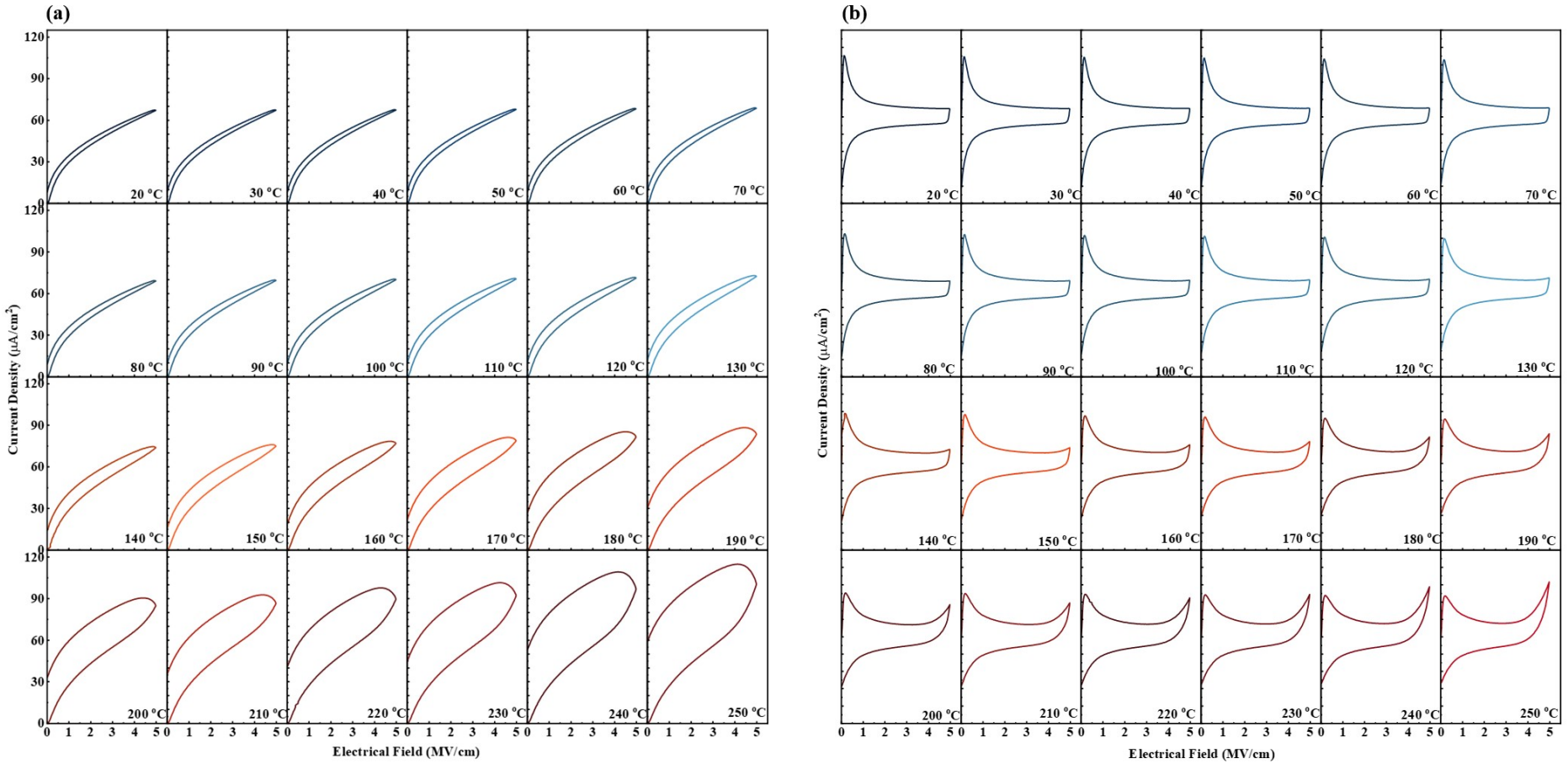


*Figure S13 The (a) P-E loops; (b) J-E curves of the BCZT-/BCZT-$_{OD}$//(1P) from room temperature to 250 $^{o}$C at 1000 Hz at 5.0 MV/cm.*

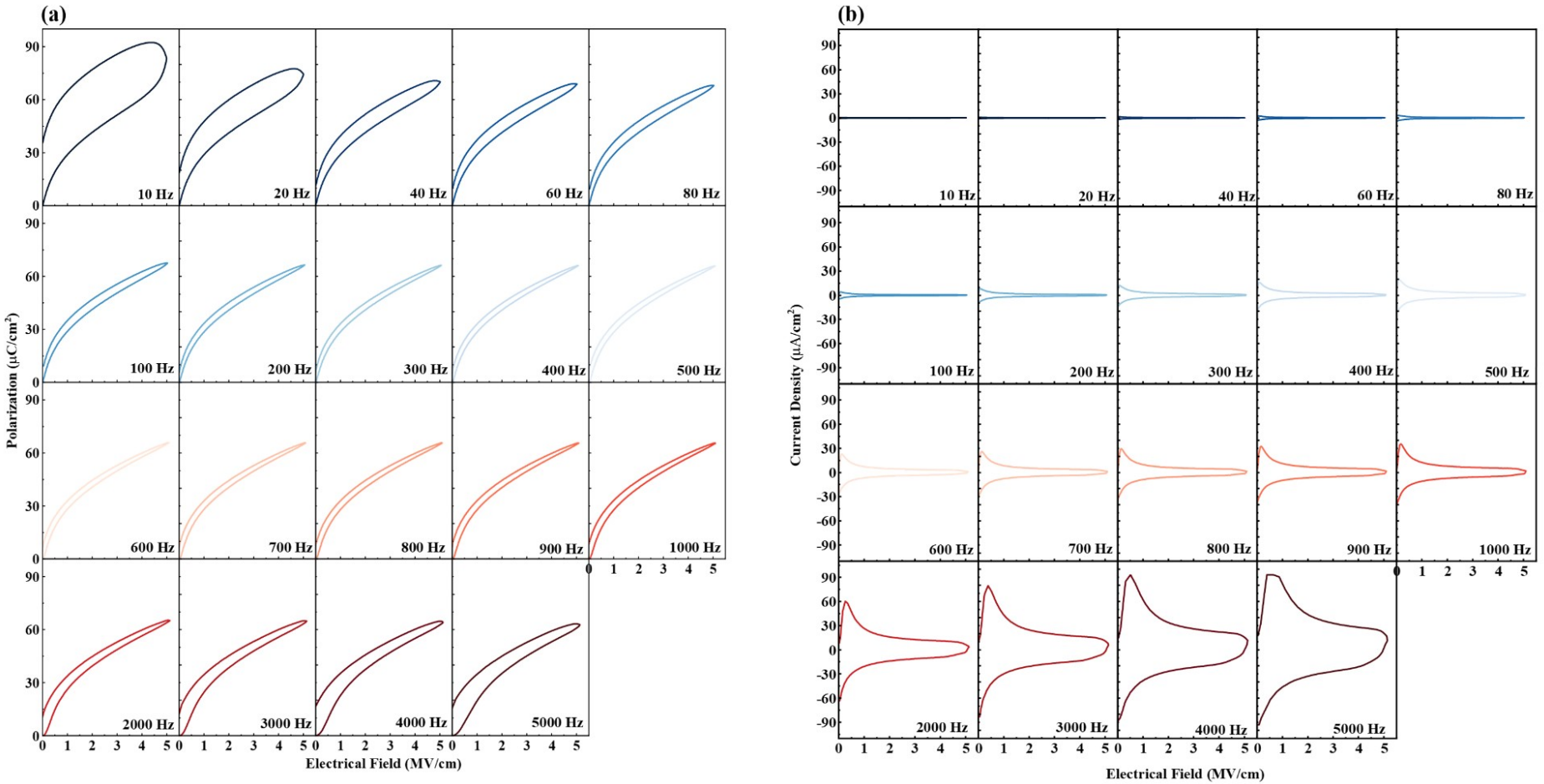


*Figure S14 The (a) P-E loops; (b) J-E curves of the BCZT-/BCZT-$_{OD}$//(1P) from room temperature to 250 °C at 1000 Hz at room temperature.*

## References


[1] S. Hirose, S. Ueda and N. Ohashi, *J. Appl. Phys.*, 2019, **125**, 10.

[2] Y. H. Wang, X. L. Shi, X. B. Lai, Z. P. Gao, L. X. Liu, Y. Wang, W. J. Zhu, C. M. Meng and L. W. Zhang, *Appl. Phys. Lett.*, 2016, **108**, 5.

[3] F. Rao, M. Kim, A. Freeman, S. Tang and M. Anthony, *Phys. Rev. B*, 1997, **55**, 13953.

[4] N. Barrett, J. Rault, I. Krug, B. Vilquin, G. Niu, B. Gautier, D. Albertini, P. Lecoeur and O. Renault, *Surf. Interface Anal.*, 2010, **42**, 1690-1694.

[5] J. Y. Dong, J. Han, Y. S. Liu, A. Nakajima, S. Matsushita, S. H. Wei and W. Gao, *ACS Appl. Mater. Interfaces*, 2014, **6**, 1385-1388.